LAWRENCE
LIVERMORE
NATIONAL
LABORATORY

LLNL-JRNL-547774

Arc-based smoothing of ion beam intensity on targets

A. Friedman

April 12, 2012

Physics of Plasmas

Disclaimer

Arc-based smoothing of ion beam intensity on targets

Alex Friedman*
Lawrence Livermore National Laboratory, Livermore, CA 94550, USA
and
The Virtual National Laboratory for Heavy Ion Fusion Science
(Dated: April 11, 2012, 14:29)

By manipulating a set of ion beams upstream of a target, it is possible to arrange for a smoother deposition pattern, so as to achieve more uniform illumination of the target. A uniform energy deposition pattern is important for applications including ion-beam-driven high energy density physics and heavy-ion beam-driven inertial fusion energy ("heavy-ion fusion"). Here, we consider an approach to such smoothing that is based on rapidly "wobbling" each of the beams back and forth along a short arc-shaped path, via oscillating fields applied upstream of the final pulse compression. In this technique, uniformity is achieved in the time-averaged sense; this is sufficient provided the beam oscillation timescale is short relative to the hydrodynamic timescale of the target implosion. This work builds on two earlier concepts: elliptical beams applied to a distributed-radiator target [D. A. Callahan and M. Tabak, *Phys. Plasmas* **7**, 2083 (2000)]; and beams that are wobbled so as to trace a number of full rotations around a circular or elliptical path [M. M. Basko, T. Schlegel, and J. Maruhn, *Phys. Plasmas* **11**, 1577 (2004).] Here we describe the arc-based smoothing approach, and compare it to results obtainable using an elliptical-beam prescription. In particular, we assess the potential of these approaches for minimization of azimuthal asymmetry, for the case of a ring of beams arranged on a cone. It is found that, for small numbers of beams on the ring, the arc-based smoothing approach offers superior uniformity. In contrast with the full-rotation approach, arc-based smoothing remains usable when the geometry precludes wobbling the beams around a full circle, *e.g.*, for the X-target [E. Henestroza, B. G. Logan, and L. J. Perkins, *Phys. Plasmas* **18**, 032702 (2011)] and some classes of distributed-radiator targets.

I. INTRODUCTION

A suitably shaped, smooth energy deposition pattern is important for applications including ion-beam-driven high energy density physics studies, and heavy-ion beam-driven inertial fusion energy (Heavy-Ion Fusion).[1–4] By manipulating a set of ion beams upstream of a target, it is possible to arrange for more uniform illumination of the target, so as to achieve a smooth deposition profile. This paper describes an approach to such smoothing that is based on rapidly "wobbling" each ion beam back and forth along a short arc-shaped path, via oscillating fields applied upstream of the final pulse compression. In this arc-based smoothing technique, uniformity is achieved in the time-averaged sense; this is sufficient provided that the beam oscillation timescale is short relative to the hydrodynamic timescale of the target implosion. This work builds on two earlier concepts: elliptical beams applied to a distributed-radiator target;[5] and beams that are wobbled so as to trace a number of full rotations around a circular or elliptical path[6–14].

In the aforementioned applications, the ion beam pulse is temporally compressed after exiting the accelerator via a process called drift compression, analogous to chirped-pulse compression of laser pulses. A head-to-tail velocity gradient, or "tilt," is imparted to the beam, which then drifts for some distance, while the beam's tail (nearly) "catches up" with its head. Two variants are possible. In the first, the beam remains un-neutralized, and the inward motion of the beam ends (in the co-moving frame) is ultimately halted by the beam's space-charge (a stagnation of the inward flow); this yields a nearly mono-energetic beam at the point of peak compression, facilitating subsequent transverse focusing by minimizing chromatic effects. Alternatively, in neutralized drift compression, the beam drifts through a plasma, wherein electrons move so as to cancel out the beam's self electric field. This enables a much shorter ion pulse, but there is no stagnation and hence the energy spread of the compressed beam is greater (as expected from Liouville's theorem). The latter variant is the basis of the new Neutralized Drift Compression Experiment-II (NDCX-II) facility at Lawrence Berkeley National Laboratory.[15]

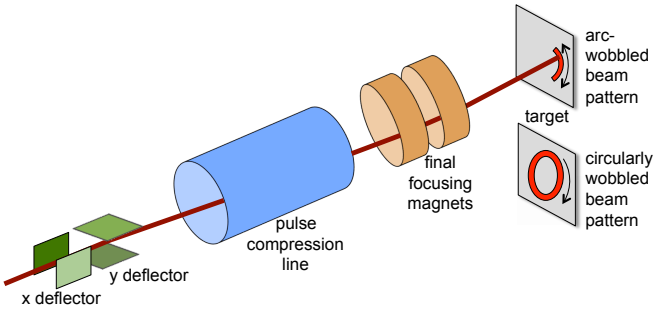

FIG. 1. Wobbler geometry, showing a single beam in the crossed-deflector system, the longitudinal bunch-compression line, the final-focus quadrupole magnet array, and impinging on the target. Both arc-wobbled and circularly-wobbled illumination patterns are shown.

Downstream of the pulse compression, the beam is focused onto the target by a final focusing system, typically a magnetic quadrupole array or a strong solenoid (plasma lenses have also been used). The temporal compression

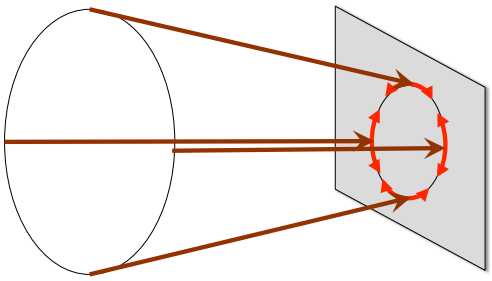

FIG. 2. (color online) Geometry of multiple beams converging onto target along a cone, showing arc-wobbled aiming points.

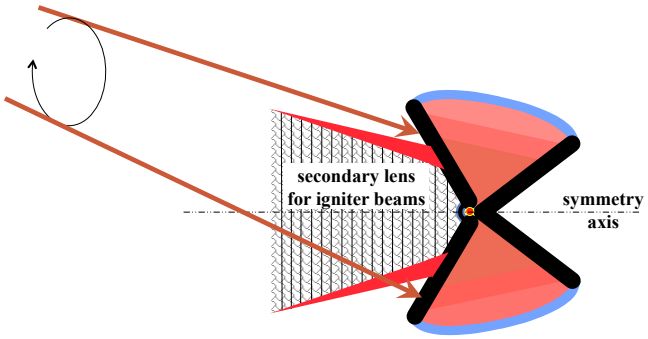

FIG. 3. (color online) Depiction of a full-circle-wobbled beam impinging upon an X-target, showing interference with the secondary-focus lens that enables focusing of a fast-ignition ion beam. Even in the absence of such a lens, the beam enters the target at an unsuitable angle when it is aimed at points on the far side of the axis of symmetry. The arc-wobbled approach avoids these issues by keeping the beam near the upper arrow in the figure.

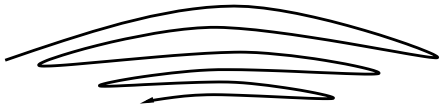

FIG. 4. Sketch of "switchback" geometry for two-harmonic wobbler approach (see text).

also serves to multiply the frequency of the oscillations imposed by the upstream wobbler, typically by factors of order ten to fifty. For example, consider a case wherein the beam pulse duration at the target is 1 ns, and ten periods of beam oscillation are desired to ensure that the oscillation period is sufficiently shorter than the implosion time. Thus, the oscillation frequency of the transverse beam motion at the target will be 10 GHz. If the beam is compressed by a factor of twenty in its travel from the wobbler to the target, the frequency of the wobbler will be 0.5 GHz. Figure 1 depicts the overall geometry of this approach, for a single beam.

Practical systems for driving inertial fusion energy targets will require tens of beams (some concepts require about 200), so the overall facility layout can be greatly simplified by arranging these beams on nested cones. Most target concepts require one such set of cones on each side of the target, but some, such as the X-target,[16] are to be illuminated from a single side. This geometry is shown in Fig. 2.

If one attempts to apply full-circle beam wobbling to the X-target, the attached "secondary" focusing lens (for the igniter beams) blocks the beam path; see Fig. 3. In addition, the angle of incidence into the target is unsuitable when (in the case shown) the beam is impinging upon the lower portion of the target, since the beam rapidly exits the target without heating enough material. This latter issue also arises with other target concepts, such as the distributed-radiator, that do not include external beam obstructions. The arc-wobbled approach remains usable with such targets.

Some targets can benefit by beam "zooming," that is, shifting the beams' aiming as the implosion proceeds. In a full-circle wobbler scenario, the amplitude of the wobbler-driven deflections may be reduced, thereby shrinking the circle on the target. For example, in a polar direct drive scenario, the aiming of beams not pointed directly at the target center can be shifted as the spherical ablation surface moves inward, thereby minimizing the beam power that fails to drive the implosion and is wasted. In an arc-wobbler scenario, a steady inward motion can be superimposed, producing a switchback geometry as shown in Fig. 4. For example, this technique may be applied to the X-target, where it is important to distribute the beam energy uniformly in the absorber, and thus avoid local depletion of absorbing material and enlargement of the ion range. The switchback is achieved by gradually reducing the amplitude of the applied field that provides the deflection along x, while ramping up a slowly varying deflection in the $-y$ direction (while retaining the second-harmonic oscillating deflection in y).

We compare the smoothness offered by the arc-based smoothing approach to that obtainable using an elliptical-beam prescription. In particular, we consider the minimization of azimuthal asymmetry, for the case of a ring of beams arranged on a cone. We have examined three variations of arc-based smoothing: wobbling the beam along straight lines; along perfect circular arcs; and along approximately circular arcs that are more readily generated by practical hardware, in a process we label "two-harmonic wobbling," described below. We find the illumination patterns from the last two prescriptions to be almost indistinguishable from each other. For small numbers of beams on the ring, the arc-based smoothing approach (with circular or near-circular arcs) offers uniformity superior to that obtainable with elliptical beams.

The layout of this paper is as follows. Section II describes the measures of nonuniformity used. Section III presents the reference elliptical beam case,[5] and a variation with less elongated beams. Section IV describes the arc-based smoothing concept, and introduces two-harmonic wobblers that yield approximately circular arcs. Section V displays a single two-harmonic arc-wobbled beam, explains how the summed effect of the set

of such beams is computed, and presents examples of the uniformity that can be obtained using arc-based smoothing. Finally, Section VI offers a discussion and considers the applicability of beam smoothing techniques to various classes of targets.

II. METRICS OF NONUNIFORMITY

For a cone of beams, the intensity pattern on a planar target surface forms an annulus, peaked at some radius and falling off at greater and lesser radii. That is, a surface plot of the intensity will resemble in appearance a volcano, while a contour plot will resemble a ring. Here we consider three measures of nonuniformity: a Fourier decomposition around the azimuth of the radially-integrated intensity; a peak-to-valley relative variation around the "rim" of the volcano, suitably defined; and a peak-to-valley relative variation of the radially integrated intensity.

For the modal metric, the $m^{\rm th}$ cosine component of the relative asymmetry in the beam energy fluence (energy passing through a unit area) is, using conventional polar (r, θ) coordinates:

$$C_m = \frac{\int_0^\infty \int_0^{2\pi} r \cos(m\theta) f[x(r,\theta), y(r,\theta)] d\theta dr}{\int_0^\infty \int_0^{2\pi} r f[x(r,\theta), y(r,\theta)] d\theta dr} \qquad (1)$$

where the above form was chosen to make explicit the fact that, in the program, the fluence f is evaluated, for each smoothing scheme, in the Cartesian coordinate space (x, y). In practice the integrals do not extend to infinity, but rather until the intensity is negligible. The sine component S_m is defined similarly.

For the peak-to-valley relative variation on the rim, we first attempted to measure the fluence at the radius of the nominal annulus (the radius of the aiming points for the elliptical beam case, or the aiming point at the middle of a "wobble" oscillation for the wobbled cases. However, when multiple beams overlap it is common that the peak intensity does not fall at that radius. Thus, we employ a search to find the location of the actual peak intensity, and (in keeping with the volcano metaphor) define the "rim" radius $r_{\rm rim}$ on which the nonuniformity is measured to be the radius of that peak. It is possible to make other choices for $r_{\rm rim}$; one that may yield a slightly more smoothly varying measure would be to integrate the intensity around θ, and define $r_{\rm rim}$ as that radius at which the result, or product of the result and the radius, is maximized.

Once a choice for $r_{\rm rim}$ has been made, the peak-to-valley relative variation at $r_{\rm rim}$ is defined as:

$$PTV_{\rm rim} = 2\frac{\max_\theta f(r_{\rm rim}, \theta) - \min_\theta f(r_{\rm rim}, \theta)}{\max_\theta f(r_{\rm rim}, \theta) + \min_\theta f(r_{\rm rim}, \theta)} \qquad (2)$$

(Note that some previous work, *e.g.*, Ref. 10, has not included, in their definition of peak-to-valley variation, the factor of 2 that appears in this definition.)

For the peak-to-valley relative variation of the radially-integrated intensity, we have:

$$f(\theta) = \int_0^\infty r f(r, \theta) dr \qquad (3)$$

$$PTV_{\rm integrated} = 2\frac{\max_\theta f(\theta) - \min_\theta f(\theta)}{\max_\theta f(\theta) + \min_\theta f(\theta)} \qquad (4)$$

III. ELLIPTICAL BEAM REFERENCE CASE

We begin with the elliptical beams described in the overview paper of Callahan and Tabak.[5] We examine the smoothness affordable by defocusing the beams along one axis, that is, stretching them along the tangent to the annulus. Originally it had been thought that this could ease the requirements on beam quality. This was a consequence of assuming that emittance could be exchanged between the transverse directions while conserving the 6-D phase space volume. This is no longer thought to be the case, though such processes as beam neutralization are likely to be eased by a reduced beam density.

In the cited work, the semimajor and semiminor axes are defined so as to contain 95% of the beam. However, an ellipse defined by semi-axes (a, b) of twice the RMS lengths contains only about 86% of the particles. Thus, for comparison with the earlier work we use an ellipse with semi-axes of 2.44775 times the RMS lengths. An iteration shows that such an ellipse contains about 95% of the particles. That is,

$$\frac{\int_0^{2.44775} 2\pi r e^{-r^2/2} dr}{\int_0^\infty 2\pi r e^{-r^2/2} dr} = 0.95 \qquad (5)$$

and $(x_{\rm RMS}, y_{\rm RMS}) = (a, b)/2.44775$. The radius of the annulus (on the end of the hohlraum) onto which the beam centroids are aimed is 3.33 mm; there is a beam-block of radius 2.0 mm, and the radius of the edge of the target is 5.0 mm.

The intensity of a single elliptical Gaussian beam is:

$$f_e(x, y) = \exp\left[-\left(\frac{x^2}{2x_{\rm RMS}^2} + \frac{y^2}{2y_{\rm RMS}^2}\right)\right]. \qquad (6)$$

For the 8-beam case of Callahan and Tabak, a=4.15 mm and b=1.8 mm. The combination of 8 such beams yields the intensity pattern of Fig. 5.

Callahan and Tabak report that the cosine-mode asymmetry in mode 8 is -1.6%. To match this, we find that we have to multiply our result for C_8 by π; omitting that scaling factor, we find the dominant components to be $C_8 = -0.0051$, $C_{16} = 0.00027$, $C_{32} = 0.00043$, $S_{16} = -0.0043$, $S_{32} = -0.0015$ and the peak-to-valley variations $PTV_{\rm rim} = 0.097$ and $PTV_{\rm integrated} = 0.020$.

Greater uniformity around the rim may be achieved by varying the semi-major axis length (a), at the expense

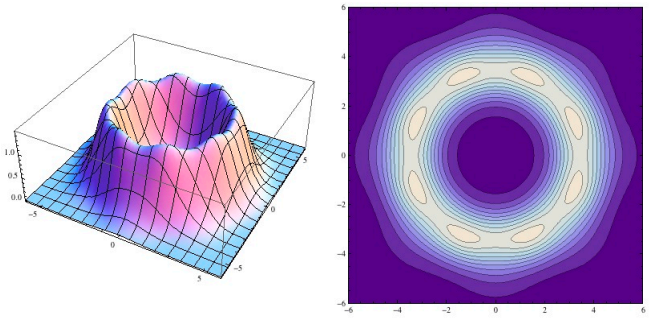

FIG. 5. Intensity pattern of 8 elliptical beams, with a=4.15 mm and b=1.8 mm. The left panel is a "mountain range" representation, while the right panel is a contour plot.

of a larger mode 8 Fourier component and greater integrated peak-to-valley nonuniformity. See Fig. 6. For a=3.14 mm, we find the dominant components to be $C_8 = -0.0091$, $C_{16} = -0.00005$, $C_{32} = 0.00078$, $S_{16} = -0.0078$, $S_{32} = -0.0031$, and the peak-to-valley variations $PTV_{\rm rim} = 0.00076$ and $PTV_{\rm integrated} = 0.037$.

When 16 beams are used, excellent uniformity can be achieved. See Fig. 7. We find the dominant components to be $C_{16} = 0.00027$, $S_{32} = 0.00023$, and the peak-to-valley variations $PTV_{\rm rim} = 0.00027$ and $PTV_{\rm integrated} = 0.0011$.

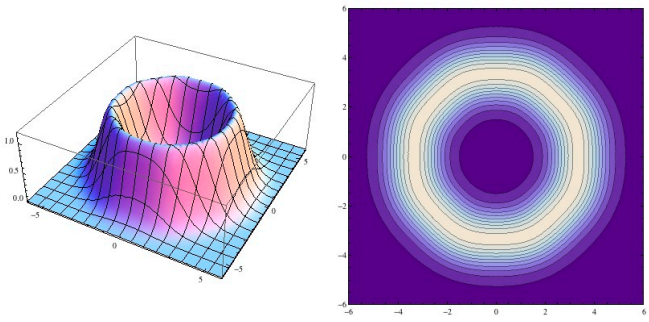

FIG. 6. Intensity pattern of 8 elliptical beams, with a=3.14 mm and b=1.8 mm.

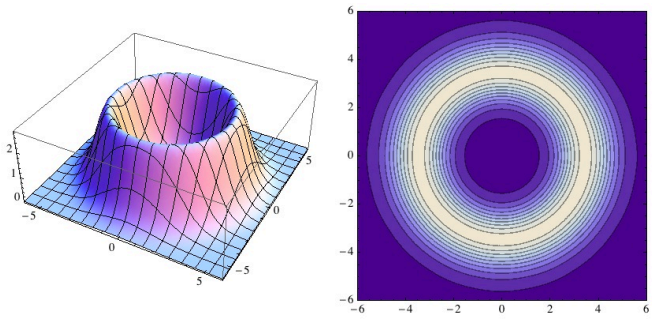

FIG. 7. Intensity pattern of 16 elliptical beams, with a=4.15 mm and b=1.8 mm.

IV. ARC-BASED SMOOTHING CONCEPT

We began by examining the process of locally wobbling a Gaussian beam back and forth. The first complication that comes to mind is that, for a harmonic oscillation, the beam will "spend more time" near its turning points than it will in mid-oscillation; thus, if the ratio of wobble amplitude to beam size is sufficiently large, one winds up with a "two humped" time-averaged distribution (in some cases, this may be acceptable). For sufficiently small wobble amplitudes, a single-humped distribution is obtained, and indeed by tuning the ratio of beam size to wobble amplitude it is possible to obtain a locally "flat" distribution (with zero second derivative at its center).

In a one-dimensional realization, the time-averaged density of the wobbled Gaussian is:

$$f(x) = \int_0^1 \exp\left[-\frac{[x - wd\cos(\pi t)]^2}{2d^2}\right] dt, \qquad (7)$$

where d is the RMS size of the unperturbed Gaussian, and w (dimensionless) is the wobble amplitude in units of d. Differentiating twice with respect to x/d yields

$$f''(0) = \frac{1}{2}e^{-\frac{w^2}{4}}\left[(w^2-2)I_0\left(\frac{w^2}{4}\right) - w^2 I_1\left(\frac{w^2}{4}\right)\right]. \qquad (8)$$

Requiring $f''(0) = 0$ and solving for the root numerically, we find a flat-topped profile for $w \simeq 1.7776$.

If we then consider the superposition of a set of n such beams offset from each other by a distance s, we find the aggregate intensity distribution $u(x)$ to be:

$$u(x) = \sum_0^{n-1} f(x - ns) \qquad (9)$$

The results of such a one-dimensional test are shown in Fig. 8, where the parameters are $d = 1$, $w = 1.75$, $s = 2$.

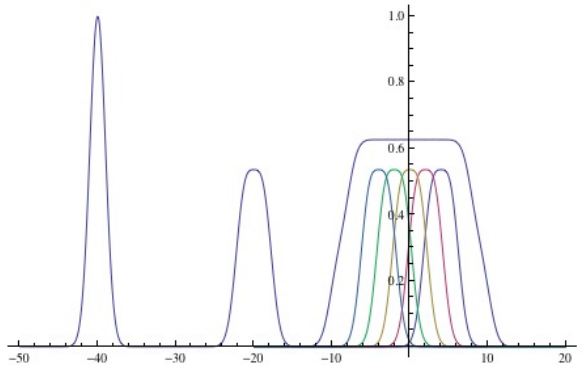

FIG. 8. One-dimensional example of locally wobbling beams, with parameters as described in the text. From left to right: the unperturbed Gaussian, a wobbled Gaussian, a set of five wobbled Gaussians positioned to overlap, and (on top of the last of these) one-half the sum of the five wobbled Gaussians.

It is evident that excellent uniformity can be obtained in this simple one-dimensional case. Similarly, we examined two-dimensional Gaussians wobbled linearly and placed side-by-side, and obtained a uniform linear profile. For brevity we do not include those results.

To explore the utility of the concept in realistic geometries, we began by considering "ideal" arc-wobbling, along perfectly circular arcs. The aiming point traces out a parametrically-defined path:

$$\begin{aligned} \text{For } -\frac{wd}{r_a} &\le \eta \le \frac{wd}{r_a}: \\ x &= r_a\cos(\eta) \\ y &= r_a\sin(\eta) \end{aligned} \tag{10}$$

where wd is the amplitude measured along the arc, η the path parameter, and r_a the arc radius. See Fig. 9.

In order to develop a practical approach, we then considered two-harmonic wobbling, wherein again the beam is deflected in the transverse (x, y) plane by RF deflector fields. However, for a two-harmonic wobbled beam, the tangential coordinate y oscillates at a base frequency ω, while the quasi-radial coordinate x oscillates at 2ω. When the deflections are applied, for each vertical cycle (up then down) that the beam completes, two horizontal cycles (left-right-left-right) are completed . The geometry is depicted in Fig. 9. In the absence of any deflections, the beam is aimed at the un-wobbled point that is called out in the figure. The equations for the aiming point are:

$$\begin{aligned} \text{For } 0 &\le t \le 1: \\ x_{\rm aim}(t) &= r_a - \frac{h}{2}[1+\cos(2\pi t)] \\ y_{\rm aim}(t) &= -r_a\sin\left(\frac{wd}{r_a}\right)\cos(\pi t) \end{aligned} \tag{11}$$

where h is the sagitta and $h/2$ is the amplitude of the "horizontal" wobble:

$$h = r_a\left[1-\cos\left(\frac{wd}{r_a}\right)\right]. \tag{12}$$

As can be seen, the aiming point traces a nearly circular arc. Furthermore, linearly wobbling the beams (along the tangent direction at mid-wobble) did not produce high-quality smoothing. Thus, for the remainder of this paper we consider only two-harmonic arc wobbling.

V. ARC-BASED SMOOTHING

Choices must be made regarding which parameters are to be considered inputs, and which derived. We specify the number of beams, the annulus radius, the ratio of wobble amplitude to spot size (thus the time-averaged shape of each wobbled beam), and the ratio of beam separation to spot size. Thus the focal spot size is, in the sequel, a derived quantity. The input parameters are:
r_a = radius of nominal aiming annulus (set to 3.33 mm)
n_b = number of beams
w = ratio of wobble amplitude to spot size d
α = ratio of beam separation s to spot size d.

The principal derived quantities are:
$s = 2\pi r_a/n_b$ = spacing of beam centers, along arc
$\Delta\phi = 2\pi/n_b$ = angular separation of beam centers
$d = s/\alpha$ = beam focal spot size $x_{\rm RMS}$.

For efficiency, we approximate the integrals over the wobble oscillation as discrete sums; tests showed that a modest number of terms suffices:
$m = 16$ = number of steps for approximate integrals
$\delta = 1/m$ = step size for approximate integrals.

Then, the time-averaged intensity of a single two-harmonic arc-wobbled Gaussian beam (for the specified number of final beams) is:

$$f_{\rm 2h}(x,y) = \delta\sum_{n=1}^{m}\exp\left[-\frac{\{x-x_{\rm aim}[(n-\frac{1}{2})\delta]\}^2+\{y-y_{\rm aim}[(n-\frac{1}{2})\delta]\}^2}{2d^2}\right] \tag{13}$$

For small numbers of beams, it can be advantageous to use a large wobble amplitude to "fill in the gaps," even though this leads to intensity peaks at the ends of the arcs. Thus, for a four-beam case we choose $w = 2.28$ and $\alpha = 6$. The derived parameters are $d = 0.8718$ mm and $s = 5.231$ mm.

A single two-harmonic arc-wobbled beam, sized as if there are to be four beams total on the annulus, then has the time-averaged intensity shown in Fig. 10.

The time-averaged intensity of n_b two-harmonic arc-wobbled beams is:

$$u_{\rm 2h}(x,y) = \sum_{i=1}^{n_b-1} f_{\rm 2h}[x\cos(i\Delta\phi)+y\sin(i\Delta\phi), \; y\cos(i\Delta\phi)-x\sin(i\Delta\phi)] \tag{14}$$

For four two-harmonic arc-wobbled beams, and the parameter choices listed above, this intensity pattern is shown in Fig. 11. The metrics for this 4-beam case, which qualitatively resembles the 8-elliptical-beam case of Fig. 5, are: $C_4 = 0.0051$, $C_8 = -0.0297$, $C_{12} = -0.0078$, $C_{16} = -0.0068$, $S_8 = 0.0024$, $S_{12} = -0.0227$, $S_{16} = -0.015$, and the peak-to-valley variations $PTV_{\rm rim} = 0.117$ and $PTV_{\rm integrated} = 0.16$. The illumination pattern is not as uniform as that of the "standard" 8–elliptical-beam case, but might well be smooth enough for a distributed-radiator target.

Moving to eight beams, it is advantageous to reduce the wobble amplitude, and we consider $w = 1.75$ and $\alpha = 2.0$. The derived parameters are $d = 1.308$ mm and $s = 2.615$ mm. The resulting intensity pattern is shown in Fig. 12.The metrics for this case correspond to significantly better uniformity than was observed for either of the 8-elliptical-beam cases presented earlier: $C_8 = -0.00006$, $C_{12} = -0.00002$, $C_{16} = -8.6\times10^{-7}$, $S_{12} = -0.00005$, $S_{16} = -0.00005$, and the peak-to-valley variations $PTV_{\rm rim} = 0.00015$ and $PTV_{\rm integrated} =$

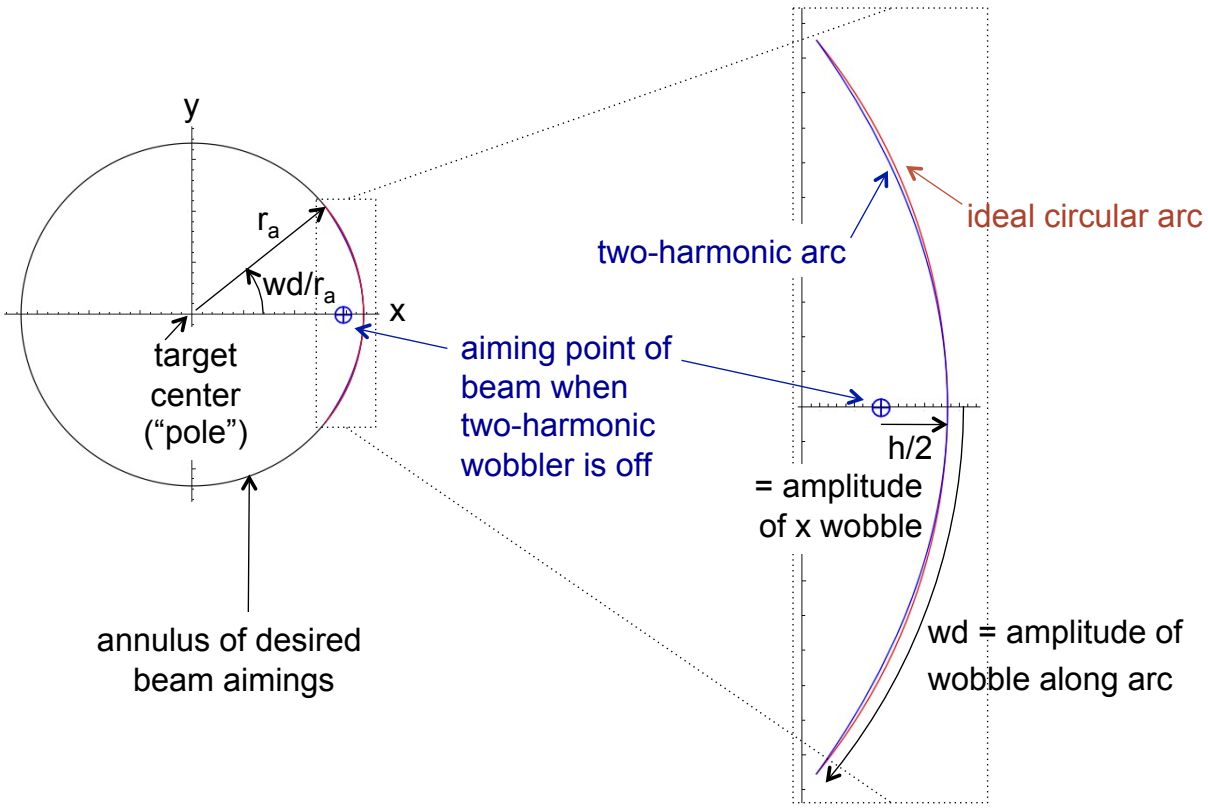

FIG. 9. (color online) Geometry of arc wobbling (see text).

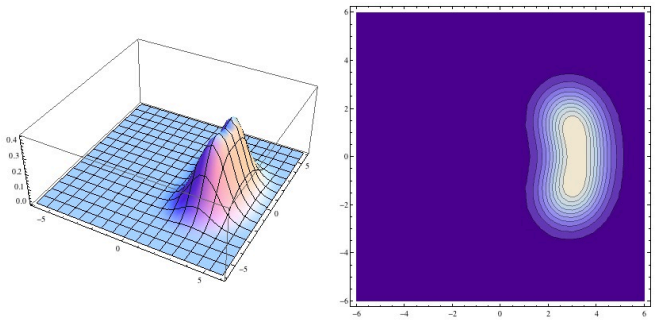

FIG. 10. (color online) Time-averaged intensity of a single two-harmonic arc-wobbled beam, one of a set of four.

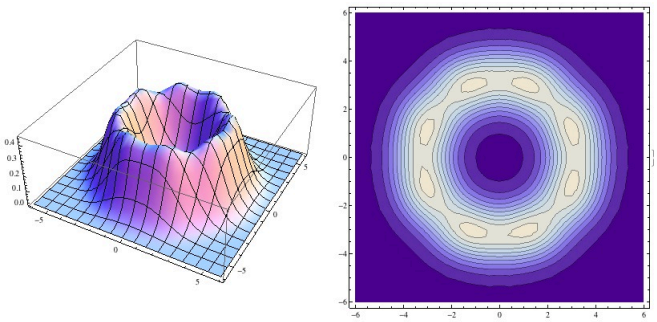

FIG. 11. (color online) The time-averaged intensity of a set of four two-harmonic arc-wobbled beams.

0.00024. These values are smaller than those observed for the case of 16 elliptical beams.

VI. DISCUSSION

In this work we have made a number of assumptions. The beams are aimed down the surface of a (virtual) cone so that their focal spots fall on a circular annular ring. The final-focusing elements are far enough upstream that the beams can be assumed to change direction only insignificantly as they are wobbled (this is generally a good approximation). The cone angle has been assumed to be very small; indeed, these studies are carried out in the limit of zero cone angle, that is, a circular cylinder. The surface on which the intensity is calculated is planar and normal to both the cone axis and the nominal axes of each of the beams (i.e., the non-wobbled axes). None of these simplifications is fundamental; any or all could be relaxed. We proceed to discuss these assumptions in the context of a number of target classes.

For *planar targets* intended for basic science studies, and for studies of ion-driven ablation for heavy-ion fusion, there is likely to be little advantage to the arc-wobbled approach, since typically a single beam is needed and, if necessary, a full-circle wobbler could be used.

For *indirect-drive distributed-radiator targets*, the assumption of a planar target surface is likely to be reason-

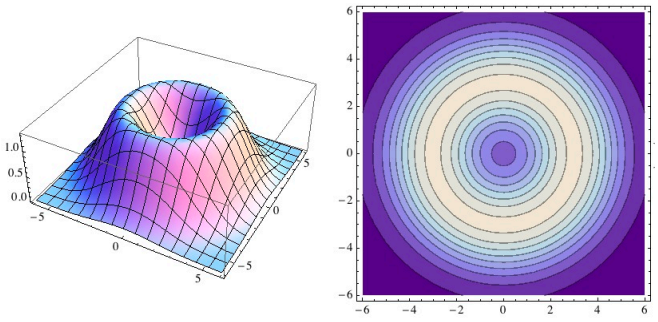

FIG. 12. (color online) The time-averaged intensity of a set of eight two-harmonic arc-wobbled beams.

able. Some correction due to the finite cone angle $\mu_{\rm cone}$ is called for, since the target surface is normal to the cone axis but not to any beam"s nominal axis. In general, for modest wobble amplitudes, this geometry will have a minimal effect on the oscillatory motion along the y coordinate in Fig. 9, but will effectively "stretch" the amplitude of the oscillation in x from $h/2$ to $h/[2\cos(\mu_{\rm cone})]$. A straightforward correction that yields a nearly circular arc on the target surface can be obtained by simply reducing, by a factor $\cos(\mu_{\rm cone})$, the strength of the field that induces the x component of the wobble.

For *the X-target*, the target surface may or may not be normal to the beams' nominal axes. A canted target, as depicted in Fig. 3, would allow normal incidence. As noted above, such a target requires additional focusing of the igniter beams, and this geometry precludes full-circle beam wobbling.

For *spherical direct-drive targets*, a distinction must be made between two cases. Kawata *et al.*[17] consider a modified Platonic-solid configuration, with 32 beams directed radially onto the face-centers and vertices of an icosahedron (case a, below). In contrast, Runge and Logan[10] consider a polar direct drive geometry with beams coming in on cones, as assumed in this paper (case b).
(a) For modified Platonic solid geometry; the un-wobbled beam centroids are normally incident, but the wobbled beam centroids are not. Here, full-rotation wobbling is an attractive approach. However, Kawata has recently described an issue with "imprinting" of early-time deposition nonuniformities, because the wobbled beams are aimed away from the on-target locations of optimal symmetry when the pulse starts. He has shown that this can be addressed by ramping up the wobbler amplitude (thus "spiraling out" the beam) over about two full rotations[12]. We conjecture that a more gradual ramping-up of the intensity might also be a useful mitigation technique.
(b) For polar direct drive geometry, the target surface may be normal to the nominal axes of the beams on one cone. However, in general, it will not be normal to the nominal axes of beams on other cones. Runge and Logan show how full-rotation wobbling can smooth the time-averaged intensity very effectively. However, they assume very rapid wobbling and consider only the integrated intensity; as Kawata notes, wobbled beams at early time will not be aimed so as to preserve the degree of symmetry inherent in the nominal (un-wobbled) aiming. Here, the arc-wobbled approach may offer an advantage, since the beams on all rings may be wobbled in synchronicity, preserving the same symmetry as that of the nominal aiming, only rotated (and with a slightly greater degree of non-normal incidence). To the extent that the points on the spherical target surface remain equidistant from the beam source as the beam travels on its arc, the equations governing that arc are unchanged from those derived herein. As mentioned earlier, "zooming" of the beam pointing is an attractive possibility.

In comparison with the full-rotation wobbler, the arc-wobbled approach, in general, involves smaller beam displacements, reducing the necessary applied deflecting fields by a modest factor along one axis, and by a substantial factor along the other. This effect is larger for greater numbers of beams.

In this work we have not attempted to model beam energy deposition into targets, including the effects of grazing incidence and beam "spill" over the target edge, because of the multiplicity of possible target geometries to which the technique might be applied. Similarly we have not addressed the influence of beam wobbling on implosion symmetry and Rayleigh-Taylor growth in targets. The full-rotation wobbler approach has been shown to have a stabilizing effect on Rayleigh-Taylor instability by oscillating the driving term. The reader is referred to Refs. 7–13 and 17 for work that bears on these issues. We may anticipate a qualitatively similar (but quantitatively different) benefit from arc-wobbling the beams.

ACKNOWLEDGMENTS

The author gratefully acknowledges helpful discussions with J. J. Barnard, E. Henestroza, H. Qin, P. A. Seidl, and M. R. Terry.

For all of this work, the Mathematica software package[18] was employed in the calculations and the display of results.

This work was performed under the auspices of the USDOE by LLNL under Contract DE-AC52-07NA27344.

* af@llnl.gov; https://www-pls.llnl.gov/fesp/hifs

[1] B. G. Logan, F. M. Bieniosek, C. M. Celata, J. Coleman, W. Greenway, E. Henestroza, J. W. Kwan, E. P. Lee, M. A. Leitner, P. K. Roy, P. A. Seidl, J.-L. Vay, W. L. Waldron, S. S. Yu, J. J. Barnard, R. H. Cohen, A. Friedman, D. P. Grote, M. Kireeff Covo, A. W. Molvik, et al., *Nucl. Instr. and Meth.* **A 577**, 1 (2007).

[2] D. H. H. Hoffmann, A. Blazevic, S. Korostiy, P. Ni, S. A.

Pikuz, B. Rethfeld, O. Rosmej, M. Roth, N. A. Tahir, S. Udrea, D. Varentsov, K. Weyrich, B. Yu. Sharkov, and Y. Maron, *Nucl. Instr. and Meth.* **A 577**, 8 (2007).

[3] B. Sharkov, *Nucl. Instr. and Meth.*, **A 577**, 14 (2007).

[4] K. Horioka, T. Kawamura, M. Nakajima, K. Kondo, M. Ogawa, Y. Oguri, J. Hasegawa, S. Kawata, T. Kikuchi, T. Sasaki, M. Murakami, and K. Takayama, *Nucl. Instr. and Meth.* **A 606**, 1 (2009).

[5] D. A. Callahan and M. Tabak, *Phys. Plasmas* **7**, 2083 (2000).

[6] B. Sharkov, N. Alexeev, M. Churazov, A. Golubev, D. Koshkarev, and P. Zenkevich, *Nucl. Instr. and Meth.* **A 464**, 1 (2001).

[7] A. R. Piriz, M. Temporal, J. J. Lopez Cela, N. A. Tahir, and D. H. H. Hoffmann, Plasma Phys. Control. Fusion 45, 1733 (2003).

[8] A. R. Piriz, N. A. Tahir, D. H. H. Hoffmann, and M. Temporal, *Phys. Rev. E* **67**, 017501 (2003).

[9] M. M. Basko, T. Schlegel, and J. Maruhn, *Phys. Plasmas* **11**, 1577 (2004).

[10] J. Runge and B. G. Logan, *Phys. Plasmas* **16**, 033109 (2009).

[11] S. Minaev, N. Alexeev, A. Golubev, D.Hoffman, T. Kulevoy, B. Sharkov, A. Sitnikov, N. A. Tahir, D. Varentsov, *Nucl. Instr. and Meth.*, **A 620** 620,99 (2010).

[12] S. Kawata, T. Kurosaki, S. Koseki, Y. Hisatomi, D. Barada, Y. Y. Ma, A. I. Ogoyski, J. J. Barnard, and B. G. Logan, "Wobbling HIB Illumination Uniformity," *Proc. 13th Japan-US Workshop on Heavy Ion Fusion and High Energy Density Physics*, Osaka University (Oct. 2011); available at http://www.nr.titech.ac.jp/JUSHIF2011/TalkSlides/J-US-HIF2011Kawata.pdf

[13] A. Bret , A. R. Piriz, and N. Tahir, *Phys. Rev. E* **85**, 036402 (2012).

[14] H. Qin, R. C. Davidson, and B. G. Logan, *Laser and Particle Beams* **29**, 365 (2011).

[15] A. Friedman, J. J. Barnard, R. H. Cohen, D. P. Grote, S. M. Lund, W. M. Sharp, A. Faltens, E. Henestroza, J.-Y. Jung, J. W. Kwan, E. P. Lee, M. A. Leitner, B. G. Logan, J.-L. Vay, W. L. Waldron, R. C. Davidson, M. Dorf, E. P. Gilson, and I. D. Kaganovich, *Phys. Plasmas* **17**, 056704 (2010).

[16] E. Henestroza, B. G. Logan, and L. J. Perkins, *Phys. Plasmas* **18**, 032702 (2011).

[17] S. Kawata, Y. Iizuka, Y. Kodera, A. I. Ogoyski, and T. Kikuchi, *Nucl. Instr. and Meth.*, **A 606**, 152 (2009).

[18] Wolfram Research, Inc., *Mathematica*, Version 8.0, Champaign, IL (2010).